Eur. Phys. J. Appl. Phys. (2016) 75: 30401
DOI: 10.1051/epjap/2016160247

THE EUROPEAN PHYSICAL JOURNAL APPLIED PHYSICS

Regular Article

Comparison of photocatalytic properties of TiO_2 thin films and fibers

Mehtap Ozdemir[1], Metin Kurt[2], Lutfi Ozyuzer[2], and Gulnur Aygun[2,a]

[1] Department of Electrical and Electronics Engineering, Gediz University, Seyrek, 35665 Izmir, Turkey
[2] Department of Physics, Izmir Institute of Technology, Urla, 35430 Izmir, Turkey

Received: 24 June 2016 / Received in final form: 10 August 2016 / Accepted: 18 August 2016

Abstract. Efficiency of solar panels degrades as a result of organic contamination such as airborne particles, bird droppings and leaves. Any foreign object on photovoltaic panels reduces the sunlight entering the absorbing surface of the solar panels. Since this leads to a major problem decreasing in energy production, solar panels should be cleaned. The self-cleaning method can be preferred. There are some methods to clean the surface of solar panels. Among the self-cleaning materials, TiO_2 is the most preferable ones because of its powerful photocatalytic properties. In this study, photocatalytic TiO_2 were produced in two different nanostructures: nanofibers and thin films. TiO_2 nanofibers were successfully produced by electrospinning. TiO_2 thin films were fabricated by reactive magnetron sputtering technique. Both TiO_2 nanofiber and thin film structures were heat-treated to form TiO_2 in anatase phase at 600 °C for 2 h in air. Then, they were evaluated by SEM analyses for morphology, X-ray diffraction (XRD) analyses for phase structures, X-ray photoelectron spectroscopy (XPS) for the chemical state and atomic concentration, and UV-spectrometer for photocatalytic performance. The results indicate that photocatalytic and transmittance properties of TiO_2 thin films are better than those of nanofibers. Consequently, TiO_2 based thin films exhibit better performance for solar cell applications due to the surface cleanliness.

1 Introduction

The amount of electric generation from solar panels is influenced by the solar radiation intensity, tilt angle of the panel surface, and surface cleanliness of cover glass [1]. Among them, the dirty surface might be due to dust accumulation [2], organic contamination (bird and other animal droppings, airborne particles, windblown dirt, water stains), organic plant matter from leaves and pollen and urban pollution (soot from burning coal or diesel) which could be prevented by various methods [3]. The contaminations reduce the amount of sunlight entering to the absorbing surface of the photovoltaic (PV) cells. Furthermore, they may be quite abrasive, scratch the surface of the solar panels and cause potential corrosion leading to permanent damage when they are not removed. As a result, the local overheating (hot spots) occurs inside the solar panels which significantly degrade the performance and lifetime [1]. Therefore, to keep the energy generation level of solar panels, the surface cleanness of the cover glass is vital [2–4]. For the same purpose, Liu et al. calculated the current loss of solar cells using transmission degradation determined with experimental data due to organic contamination [4].

There are some methods such as natural, mechanical, electrostatic and self-cleaning thin film to get rid of cleaning problems [5]. Natural methods are wind power, gravitation and rainwater, but not much effective, since their control is not possible. Mechanical methods such as wiping by brush lead to a damage on the surface. In electrostatic methods, the repulsive forces between the like charged particles are effective but this method does not work when the weather is rainy. For this reason, they cannot be effectively used in PV systems. As a result, self-cleaning method is the most efficient way to keep the surface clean.

TiO_2 is known to have three natural polymorphs, i.e., rutile, anatase and brookite [6,7]. Among them, anatase TiO_2 is commonly used for self-cleaning purposes because of its hydrophilicity and photocatalytic activity [6]. The self-cleaning method consists of two stages: photocatalytic and hydrophilic [5]. TiO_2 film reacts and decomposes the organic dirt under the ultraviolet light in photocatalytic process. Then, the rainwater will diffuse to the whole surface and rinse the dust because of its hydrophilic properties. Most researchers focus on improving the photocatalytic properties by doping with various metal ions [8–13]

[a] e-mail: gulnuraygun@iyte.edu.tr

and with different structures [14–16]. Extensive studies have been done on doping effect on the photocatalytic properties; however, little attention has been paid on the TiO_2 structural influence on the photocatalytic performance. In addition to the significance of TiO_2 in photocatalytic application, its high optical transmittance and high refractive index make it applicable in many areas such as coatings, optical filters, integrated optical chemical sensors, and optical waveguides [17].

In this study, the influence of nanofiber and thin film structure on the photocatalytic activity of TiO_2 was reported. TiO_2 nanofibers were produced with electrospinning technique while TiO_2 thin films were fabricated using magnetron sputtering technique. Photocatalytic performance was evaluated with degradation of methylene blue (MB), under illumination of visible light. Structural analysis was performed by X-ray diffraction (XRD) and surface morphology was investigated by scanning electron microscopy (SEM). Photocatalytic and transmittance properties were studied by spectrophotometer. The chemical state and atomic concentration were determined by X-ray photoelectron spectroscopy (XPS).

2 Experimental

2.1 Nanofiber production

In the electrospinning process, firstly a viscous sol was prepared [18]. The preparation of TiO_2 precursor solution was carried out under atmospheric conditions at room temperature. Titanium isopropoxide was mixed with acetic acid and ethanol, and then the solution was stirred at 25 °C for 10 min in air. After the preparation of transparent solution, the polyvinylpyrrolidone (PVP) dissolved in ethanol was added to as-prepared solution and the mixture was constantly stirred at 25 °C for 2 h. In order to produce the nanofibers, Ti-based solution was immediately loaded into a plastic syringe. The emitting electrode from a power supply was attached to the needle. The grounding electrode was attached to a piece of aluminum foil used as the collector plate and was placed approximately 8 cm below the tip of the needle. A 15 kV high voltage was applied between the needle and the collector. While jet was accelerated from the tip of the needle towards the collector, the solvent was evaporated by leaving only ultrathin fibers on soda-lime glasses (SLG) located on aluminum foil. The fabricated nanofibers were left to allow the completion of hydrolysis of titanium isopropoxide for approximately 2 h, and consequently, subjected to calcination at a high temperature of 600 °C to remove residual PVP and obtain the anatase phase.

2.2 Thin film preparation

TiO_2 thin films were deposited under high vacuum on SLG substrates by DC magnetron sputtering technique. The sputtering was done using a Ti target at room temperature. Before deposition, the substrates were cleaned in ultrasonic cleaner using acetone, ethyl alcohol and de-ionized water, respectively, for 5 min. Then, they were exposed to plasma cleaner for 10 min. When the vacuum chamber was evacuated below 10^{-6} Torr, 5 min presputtering of Ti target and 30 min deposition was carried out under 36 sccm Ar and 4 sccm O_2 atmosphere. The working gas pressure, the distance between the target and substrate, and the sputtering power were 3 mTorr, 13 cm, and 150 W, respectively. The film thicknesses were measured about 53 nm by profilometer. TiO_2 films were annealed at 600 °C for 2 h in air ambient to enhance the crystallization.

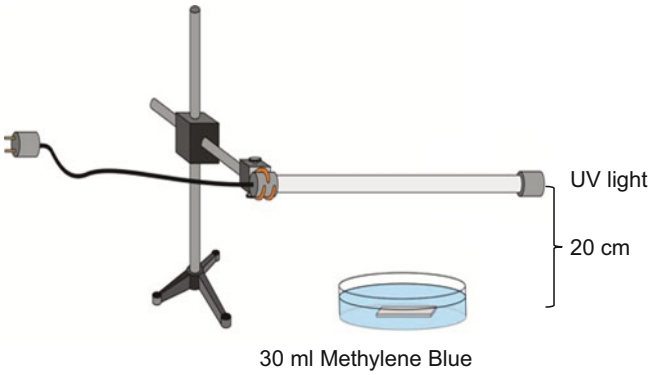

Fig. 1. Schematic representation of photocatalytic experiment setup.

2.3 Photocatalytic activity measurements

Photocatalytic degradation experiments of the specimens were carried out using a setup (Fig. 1) including aqueous methylene blue (MB) solutions for all catalysts and a UV light source (Philips, TUV, 16 W) [14–16]. MB is a common heterocyclic aromatic dye and is generally used as a model for organic compound to determine photocatalytic activity [8]. Firstly, MB precursor powder (Merck) was solved with deionized water to obtain 1×10^{-5} M MB solution. In order to record catalyst-free degradation of MB under UV radiation, a reference solution was also prepared. The MB solutions were poured into the beakers and were placed under UV-light source with a distance of approximately 20 cm. Nanofiber and thin film TiO_2 were immersed in 30 mL MB solution and 30 mL MB reference solution were left for 6 h under UV illumination. Their absorbance properties were investigated by using UV-spectrophotometer.

2.4 Material characterization

X-ray diffraction (XRD; Phillips X'Pert Pro X-ray diffractometer) was used to determine the structure of the TiO_2 fibers and films. The field emission scanning electron microscope (SEM; FEI-QuantaFEG 250) was used to observe the surface morphologies. The chemical state and atomic concentration were determined by X-ray photoelectron spectroscopy (XPS; SPECS Phoibos 150 3D-DLD). Photocatalytic and transmittance properties were

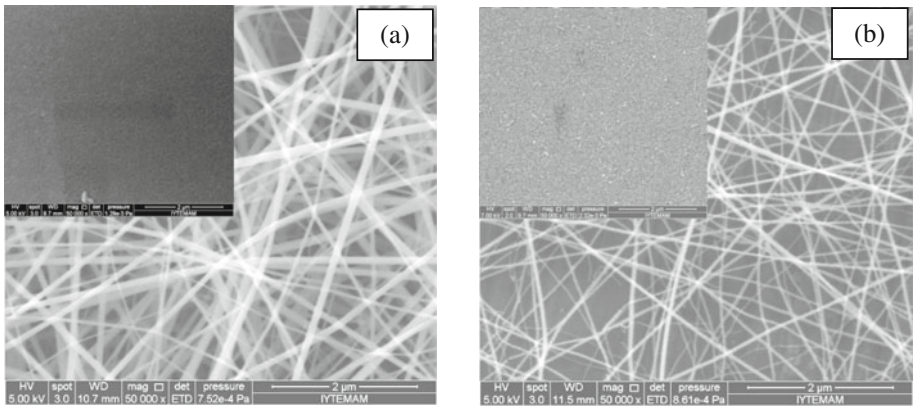

Fig. 2. SEM images of TiO_2 as grown nanofibers (a), nanofibers annealed at 600 °C (b). The inset of (a) corresponds to as grown thin film while the inset of (b) corresponds to annealed thin films at 600 °C.

investigated using UV-vis spectrometer (Perkin Elmer, Lambda 950).

3 Results and discussion

Figure 2 shows the plane-view SEM images of nanofibers and thin film grown on SLG before and after annealing process at 600 °C for 2 h. The diameters of nanofibers were quantitatively evaluated using their high magnification SEM images. Each individual nanofiber was uniform in cross section and the average diameter was 260 nm before and 180 nm after annealing (Figs. 2a and 2b). After annealing, due to the removal of organic substances in the as-spun nanofibers, the diameter of nanofibers decreased. Inset of Figures 2a and 2b show SEM images of thin film surfaces before and after heat treatment at 600 °C for 2 h. TiO_2 thin films, in general speaking, showed quite smooth surfaces with no cracks when compared to fiber structures on glass. Grain structure can be easily seen from these SEM images because of increased crystallization after annealing.

The photocatalytic activity of TiO_2 depends on the preparation technique, crystalline structure, annealing temperature, specific surface area and so on [19]. For the photocatalytic properties, the most important step of the research is to obtain TiO_2 with anatase phase [20]. According to XRD patterns as shown in Figure 3, it was found that the obtained TiO_2 nanofibers contain anatase and rutile phases even when the annealing temperature was 600 °C for 2 h in air ambient. Volume fractions of fibers were calculated by integrating the area under each peak from the XRD spectra. The volume fractions of anatase and rutile in the fibers were calculated as 0.60 and 0.40, respectively. Especially, anatase phase of pure TiO_2 having tetragonal structure was strongly observed at 600 °C as explained in literature [21–24]. It has been well known that anatase phase of TiO_2 is thermally less stable than rutile phase and transfers into rutile phase at higher temperature. It can be seen that the peaks at 2θ of 25.28, 38.08, 44.52, 47.92, 53.32 and 62.66 are assigned to (1 0 1), (0 0 4), (1 1 2), (2 0 0), (1 0 6) and (2 1 5) lattice

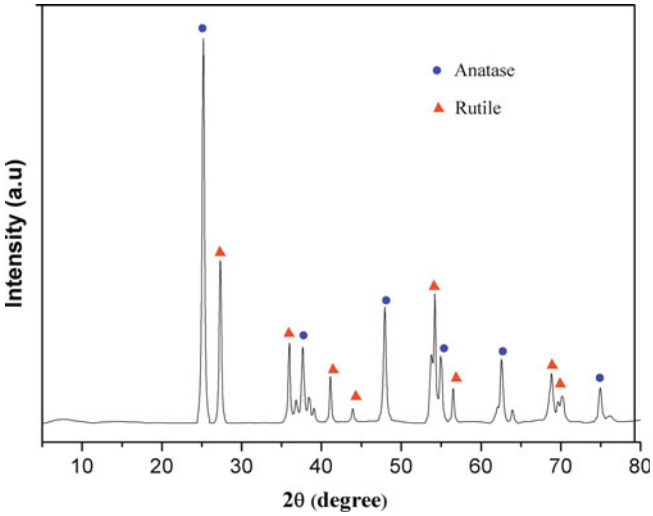

Fig. 3. The X-ray diffraction patterns of TiO_2 nanofiber annealed at 600° for 2 h.

planes of TiO_2. We have similar results with those of Jiang et al. [24] and Wang et al. [25] regarding as TiO_2 peaks. Since the thickness of thin film is too low for X-ray diffraction, XRD pattern was not obtained. On the other hand, it is clearly understood from XPS analysis that the film has anatase phase (Fig. 4).

Figure 4 shows XPS of Ti $2p$ for annealed nanofibers and thin film. It is seen that the core levels of Ti $2p_{1/2}$ and Ti $2p_{3/2}$ are located at approximately 462.8 and 457.1 eV for anatase phase and 463.0 and 457.8 eV for rutile phase for TiO_2 nanofiber (Fig. 4a). The core levels of Ti $2p_{1/2}$ and Ti $2p_{3/2}$ are located at 463.8 and 458.1 eV (Fig. 4b), respectively, for TiO_2 thin film. The spin orbit splitting between the Ti $2p_{1/2}$ and $2p_{3/2}$ core levels are 5.7 eV, indicating a normal state of Ti^{4+} in the anatase TiO_2. The core levels of Ti $2p_{1/2}$ and Ti $2p_{3/2}$ are similar to the literature data [26,27].

Figure 5 indicates the deconvolution of O $1s$ peaks for core levels of annealed TiO_2 nanofibers and thin film. Oxygen is a common contaminant in titanium surfaces because of its high oxygen affinity [25]. The O $1s$ spectrum

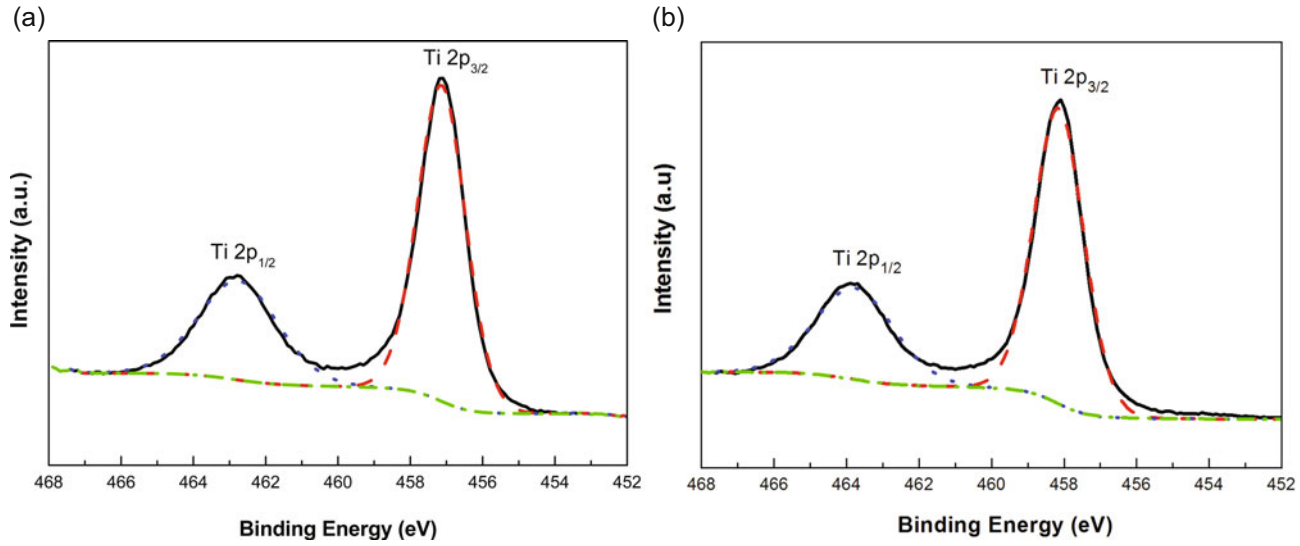

Fig. 4. X-ray photoelectron Ti 2*p* spectra of (a) TiO_2 nanofiber (b) TiO_2 thin film.

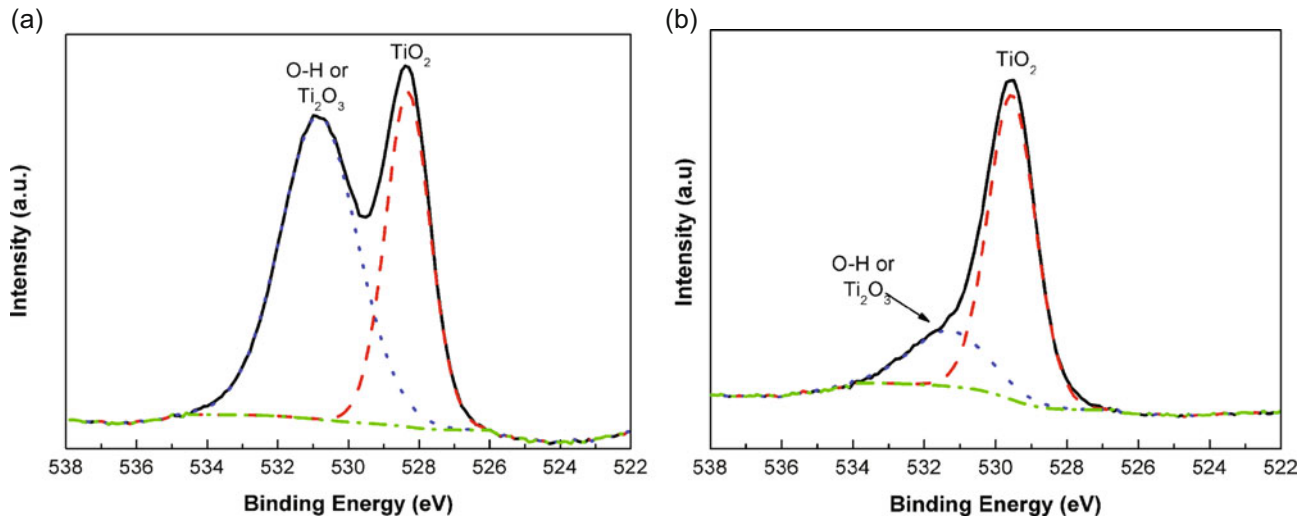

Fig. 5. X-ray photoelectron O 1*s* spectra of annealed (a) TiO_2 nanofiber (b) TiO_2 thin film.

consists of two peaks for nanofibers: the one at 528.3 eV of TiO_2 and the other at 530.8 eV for adsorbed water or fraction of Ti_2O_3 (Fig. 5a). Similarly, O 1*s* spectrum for thin film consists of two peaks located at 529.5 eV and 531.3 eV, respectively indicating to, TiO_2 and adsorbed water or Ti_2O_3 (Fig. 5b). As seen in Figure 5, the intensity coming from the adsorbed water or Ti_2O_3 is higher for fiber when compared to thin film. Since the fiber was produced from the chemical solutions, the amount of oxygen is higher, on the other hand, thin films were grown in high vacuum conditions. Therefore, when we compare the XPS spectrum of both films, fiber has a higher oxygen bonds with surroundings and OH peaks. Moreover, since the fiber structure on glass has larger surface area, it probably absorbs more water. Therefore, this results higher OH peaks in XPS spectrum in fiber structures when compared to thin film TiO_2.

Figure 6 illustrates the UV visible spectra of annealed TiO_2 thin films and nanofibers in the wavelength range from 200 to 2600 nm. The transmissivity curve of thin film TiO_2 is compatible with the literature [28]. However, it can be seen that the structure of material affects the distribution of transmissivity curves. The transmissivity in the wavelength range from 480 to 660 nm of thin film's coating is higher than that of the nanofibers' coating. This range of wavelength corresponds to visible light of electromagnetic spectrum which is very important region for solar cell applications. Moreover, the efficiency of crystalline silicon solar cells drops with increasing temperature, the lower infrared transmission of TiO_2 thin film prevents the solar cell from heating. As it is seen from the inset of Figures 2a and 2b, thin films have smooth, dense and uniform surfaces when compared to fiber structures on glass, as a result less light scattering occurs on

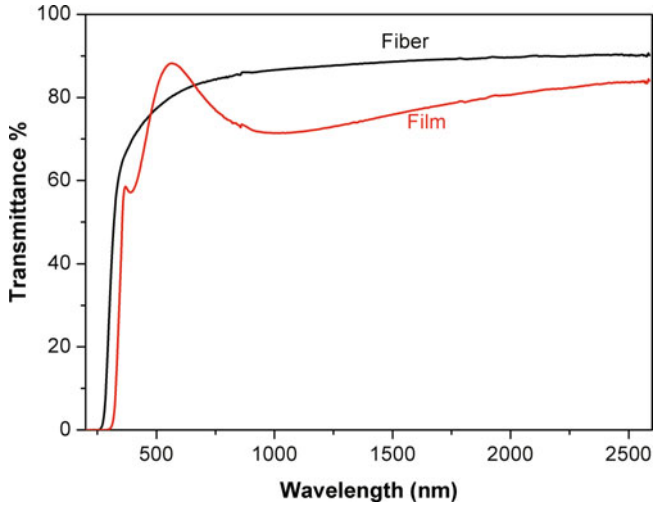

Fig. 6. Transmission spectra of annealed TiO_2 thin film and nanofibers.

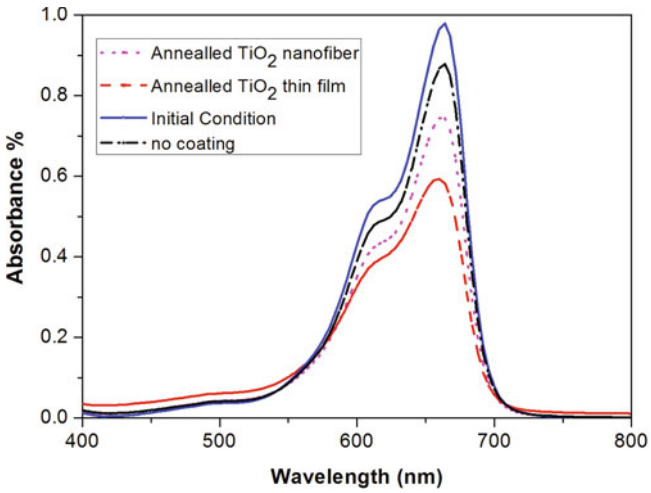

Fig. 7. Photocatalytic degradation of (a) initial MB solution (10^{-5} M), (b) UV illuminated MB solution, (c) UV illuminated MB solution with annealed TiO_2 nanofibers coating and (d) UV illuminated MB solution with annealed TiO_2 thin film.

the surface leading to a high transmittance level in visible range. Furthermore, deposited thin films of TiO_2 are very thin when compared to fibers which increase transmissivity. From the graphs; it can be easily understood that the transmittance of all samples is higher than 75%, which can fulfill the transmitting requirement of cover layer in solar cell applications [29]. Transmissivity at longer wavelength region of nanofiber is higher than that of the thin film but, according to the antireflection theory, the low transmissivity may be adjusted by altering the thickness of the layers for other applications [6].

The photoactivity of annealed thin film catalyst was determined by photo-oxidation of MB. Figure 7 shows the absorption of initial MB solution (10^{-5} M), UV illuminated MB solution, UV illuminated MB solution with annealed TiO_2 nanofibers coating and UV illuminated MB solution with annealed TiO_2 thin film, respectively. Generally, all solutions including MB show characteristic absorption band at 665 nm [23]. Besides, the aqueous solution of MB molecules exhibited another peak at 611 nm. These peaks correspond to monomers and dimers, respectively [30]. Because of the fact that the degradation rate of monomers is much higher than that of dimers, the peak at 665 nm higher than the peak at 611 nm [31]. It is inferred that the concentration decreases because of the photocatalytic degradation of the TiO_2 coatings. It can be understood that TiO_2 thin film exhibits very active behavior for photocatalytic decomposition because absorption of the solution is much lower when compared to the others. It is known that photocatalytic activity of the anatase form is known to exhibit excellent photocatalytic activity when compared with the rutile form of TiO_2. Crystallinity of the thin film cannot be obtained from XRD results, but XPS data show the spin orbit splitting between the Ti $2p_{1/2}$ and Ti $2p_{3/2}$ core levels indicating a normal state of Ti^{4+} in the anatase TiO_2. In addition, the uniformity of the surface affects the photocatalytic activity. SLG covered with thin film produced by magnetron sputtering technique is obtained more homogenously compared to nanofibers by electrospinning method. Besides, the TiO_2 nanofibers have bigger surface areas than TiO_2 thin film, they can, theoretically, be assumed to have higher photocatalytic property. However, fibers can conglomerate during the fabrication process on SLG. Therefore, the absorption of the layer is not improved [15].

4 Conclusion

In summary, we compared the properties of TiO_2 nanofibers and thin film formation. Titanium dioxide thin films with 53 nm thick via magnetron sputtering and nanofibers with 180 nm diameter by electrospinning methods were successfully fabricated. We showed that thin film's transmissivity, a very important property for solar cell applications in the visible light region, is higher than that of the nanofiber coatings. As it is well known that, TiO_2 in anatase phase is vital for photocatalytic applications. In our work, the presence of the anatase phase was confirmed with XRD and XPS analyses for annealed nanofibers and thin film samples. Their photocatalytic properties were analyzed by the degradation of 1×10^{-5} M methylene blue organic dye. Having enhanced crystallization after annealing at 600 °C, TiO_2 thin films have higher photocatalytic activity when compared to the nanofibers. Here, we have proved that magnetron sputtered grown thin films, opposite to the literature work [14], have higher photocatalytic efficiency. As a result, magnetron sputtered grown thin films are very convenient for solar cell applications.

The authors would like to thank the Applied Quantum Research Center of IZTECH (AQuReC) for the research facilities it offers for the current study.

References

1. http://www.pveducation.org/pvcdrom/properties-sunlight/solar-radiation-tilted-surface, 2016
2. H.K. Elminir, A.E. Ghitas, R. Hamid, F. El-Hussainy, M. Beheary, K.M. Abdel-Moneim, Energy Convers. Manage. **47**, 3192 (2006)
3. S. Mekhilef, R. Saidur, M. Kamalisarvestani, Renew. Sust. Energ. Rev. **16**, 2920 (2012)
4. D.L. Liu, S.H. Liu, C.J. Panetta, K.R. Olson, S.M. Hong, D.R. Alaan, C.J. Mann, K.T. Luey, in *Photovoltaic Specialists, IEEE Conference – PVSC, Honolulu, HI* (IEEE, New York, NY, 2010), p. 2563
5. G. He, C. Zhou, Z. Li, Procedia Engineering **16**, 640 (2011)
6. Z. Wang, N. Yao, X. Hu, Vacuum **108**, 20 (2014)
7. C.H. Heo, S.B. Lee, J.H. Boo, Thin Solid Films **475**, 183 (2005)
8. M. Ratova, P. Kelly, G. West, I. Iordanova, Surf. Coat. Technol. **228**, 544 (2013)
9. A. Manole, M. Dobromir, M. Gîrtan, R. Mallet, G. Rusu, D. Luca, Ceram. Int. **39**, 4771 (2013)
10. D. Dvoranova, V. Brezova, M. Mazúr, M.A. Malati, Appl. Catal. B Env. **37**, 91 (2002)
11. B. Tryba, M. Piszcz, A. Morawski, TOMSJ **4**, 5 (2010)
12. S. Bagwasi, B. Tian, J. Zhang, M. Nasir, Chem. Eng. J. **217**, 108 (2013)
13. H. Jiang, L. Gao, Mater. Chem. Phys. **77**, 878 (2003)
14. Z. Tian-Hui, P. Ling-Yu, Z. Su-Ling, X. Zheng, W. Qian, K. Chao, Chin. Phys. B **21**, 118401 (2012)
15. S.J. Doh, C. Kim, S.G. Lee, S.J. Lee, H. Kim, J. Hazard. Mater. **154**, 118 (2008)
16. U. Diebold, Surf. Sci. Rep. **48**, 53 (2003)
17. M. Yamagishi, S. Kuriki, P. Song, Y. Shigesato, Thin Solid Films **442**, 227 (2003)
18. M. Özdemir, E. Çelik, Ü. Cöcen, Mater. Technol. **47**, 735 (2013)
19. S. Ulucan, G. Aygun, L. Ozyuzer, M. Egilmez, R. Turan, J. Optoelectron. Adv. Mater. **7**, 297 (2005)
20. S. Zheng, T. Wang, G. Xiang, C. Wang, Vacuum **62**, 361 (2001)
21. M.D. Stamate, Appl. Surf. Sci. **218**, 318 (2003)
22. A. Benyoucef, A. Benyoucef, F. Lapostolle, D. Klein, B. Benyoucef, in *Revue des Energies Renouvelables ICRESD-07, Tlemcen, 2007*, p. 61
23. Y.C. Lee, Y.P. Hong, H.Y. Lee, H. Kim, Y.J. Jung, K.H. Ko, H.S. Jung, K.S. Hong, J. Colloid Interface Sci. **267**, 127 (2003)
24. X. Jiang, G. Ding, L. Lou, Y. Chen, X. Zheng, Catal. Today **93**, 811 (2004)
25. Y.M. Wang, H.C. Lin, C.C. Yen, Thin Solid Films **515**, 1047 (2006)
26. F.M. Liu, T.M. Wang, Appl. Surf. Sci. **195**, 284 (2002)
27. M. Grodzicki, R. Wasielewski, P. Mazur, S. Zuber, A. Ciszewski, Optica Applicata **43**, 99 (2013)
28. F. Meng, X. Song, Z. Sun, Vacuum **83**, 1147 (2009)
29. Y. Xiong, H. Tao, J. Zhao, H. Cheng, X. Zhao, J. Alloys Compd. **509**, 1910 (2011)
30. C. An, S. Peng, Y. Sun, Adv. Mat. **22**, 2570 (2010)
31. R. Zuo, G. Du, W. Zhang, L. Liu, Y. Liu, L. Mei, Z. Li, Adv. Mater. Sci. Eng. **2014**, 1 (2014)